Atmos. Chem. Phys. Discuss., 13, 30143–30186, 2013
www.atmos-chem-phys-discuss.net/13/30143/2013/
doi:10.5194/acpd-13-30143-2013

Atmospheric Chemistry and Physics Discussions
Open Access

Evaluation of IASI derived dust aerosols characteristics over the tropical belt

V. Capelle[1], A. Chédin[1], M. Siméon[1], C. Tsamalis[1,2], C. Pierangelo[3], M. Pondrom[1], R. Armante[1], C. Crevoisier[1], L. Crepeau[1], and N. A. Scott[1]

[1]Laboratoire de Météorologie Dynamique, UMR8539, CNRS/IPSL, Ecole Polytechnique, Palaiseau, France
[2]Met Office, Exeter, UK
[3]Centre National d'Etudes Spatiales, Toulouse, France

Received: 29 October 2013 – Accepted: 5 November 2013 – Published: 18 November 2013

Correspondence to: A. Chédin (chedin@lmd.polytechnique.fr)

Published by Copernicus Publications on behalf of the European Geosciences Union.

Abstract

IASI-derived monthly mean infrared (10 µm) dust aerosol optical depth (AOD) and altitude are evaluated against ground based AERONET measurements of the 500 nm coarse mode AOD and CALIOP measurements of the altitude at 38 AERONET sites within the tropical belt (30° N–30° S). The period covered extends from July 2007 to December 2012. The evaluation goes through the analysis of Taylor diagrams and box and whiskers plots, separating situations over sea and over land. Concerning AOD, the overall correlation for the sites over sea comes to 0.88 for 713 items (IASI and AERONET monthly mean bins). The overall normalized standard deviation is of 0.96. Over land, essentially desert, correlation is of 0.74 for 582 items and the normalized standard deviation is of 0.87. This slight but significant degradation over land most probably results from the greater complexity of the surface (heterogeneity, elevation) and, to a lesser extent, to the episodic presence of dust within the boundary layer (particularly for sites close to active sources) to which IASI, as any thermal infrared sounder, is poorly sensitive contrary to AERONET. Concerning altitude over sea, correlation is of 0.78 for 925 items and the normalized standard deviation is of 1.03. Results over land, essentially over deserts, are not satisfactory for a majority of sites. To the reasons listed above for the AOD must be added the smaller IASI signal induced by the altitude compared to the signal induced by the AOD. Site by site, disparities appear that we estimate being principally due to either the insufficient number of AERONET observations throughout the period considered, to the complexity of the situation mixing several aerosol types (case of the Persian Gulf, for example), to surface heterogeneities (elevation, emissivity, etc.), or to the use of a single aerosol model (“MITR”). Results using another aerosol model with different refractive indices are presented and discussed. We conclude that the present results demonstrate the usefulness of IASI data as an additional constraint to a better knowledge of the impact of aerosols on the climate system.

ACPD
13, 30143–30186, 2013

V. Capelle et al.

1 Introduction

During the past decades, determination of atmospheric aerosol characteristics from space has been extensively done using instruments measuring in the visible part of the spectrum. This has greatly contributed enhancing knowledge of the aerosol impact on the Earth radiation balance (direct effect) as well as on the clouds (albedo, lifetime) (indirect effect). However, these processes are complex as they involve the aerosol distribution (spatial, in particular vertical, and temporal), and their microphysical and optical properties (size, shape, composition, etc.). Moreover, the accuracy obtained on the atmospheric radiative effect also depends on surface characteristics (albedo, temperature). This complexity still leads to large uncertainties in the estimation of aerosols impact on climate (Forster et al., 2007; US Climate Change Science Program, 2009; Hansen et al., 1997; Kaufman et al., 1997; Haywood and Ramaswamy, 1998; Claquin et al., 1998; Sokolik and Toon, 1999; Myhre and Stordal, 2001; Tanré et al., 2003; Yu et al., 2006; Otto et al., 2007; Müller et al., 2012; Ryder et al., 2013).

After a long period of relative disinterest in aerosol remote sensing in the infrared (one of the oldest reference is by Legrand et al., 1989), a marked growing interest in the infrared is now observed with the emergence of hyperspectral instruments as AIRS and IASI (Pierangelo et al., 2004, 2005; De Souza-Machado, 2006; Peyridieu et al., 2010; Klüser et al., 2011, 2012; Peyridieu et al., 2013). Aerosols in the coarse mode, as dust or sea salt, have a high impact in the infrared when aerosols more typical of pollution or biomass burning usually have smaller size and affect less infrared radiation. Sea-salt particles usually remain in the bottom of the planetary boundary layer, which prevents them to have an impact on infrared radiances collected at satellite level. Most of mineral dust aerosol mass is composed of particles in the coarse size mode, thus with a potentially high optical depth in the infrared, and can be brought to high altitudes in the atmosphere, for example in the so-called Saharan Air Layer (Chiapello et al., 1995, 2005; Tsamalis et al., 2013). Consequently, the remote sensing of aerosols in the longwave domain mostly focuses on retrievals of mineral dust

ACPD
13, 30143–30186, 2013

properties (Pierangelo, 2013). This domain offers some unique opportunities such as nighttime aerosol observation, the determination of the aerosol layer mean altitude or the aerosol characterization over deserts. Mineral dust is a major contributor to total aerosol loading and has been the subject of an increasing number of studies (e.g. Maher et al., 2010; Mahowald et al., 2010; Formenti et al., 2011; Shao et al., 2011; Knippertz et al., 2012) due, in particular, to its potentially large contribution to atmospheric radiative forcing (Markowicz et al., 2003; Vogelman et al., 2003; Otto et al., 2007). However, the domain remains largely unexplored and is still poorly understood. Particles in the coarse mode are less efficient in their interaction with visible wavelengths and their association with infrared wavelengths should lead to an improvement of our knowledge of their impact on climate. This requires validating infrared-derived aerosol properties using well recognized, accurate and independent, measurements of these properties, as well as understanding possible differences brought by such comparison.

In this study, IASI-derived dust 10 µm AOD, for the period July 2007–December 2012 (Peyridieu et al., 2013), are first evaluated using accurate measurements routinely made and distributed by the Aerosol RObotic NETwork of sun-photometers (AERONET, Holben et al., 1998) for 38 sites in the tropical band. In this approach, use is made of the 500 nm coarse mode AOD from the Spectral Deconvolution Algorithm (SDA) (O'Neill, 2003). Then, around the same 38 AERONET sites, IASI-derived altitude is evaluated using observations of the two-wavelength depolarization lidar CALIOP onboard the satellite CALIPSO (Winker et al., 2007).

IASI, AERONET, and CALIOP data, are described in Sect. 2. Section 3 describes the method followed for evaluating IASI results, based on the use of Taylor diagrams (Taylor, 2001) and box and whiskers plots. Section 4 presents the results of the evaluation. In this section is also discussed the impact of the choice of infrared refractive index model made in this study. Results of this evaluation are discussed in Sect. 5.

2 Data

2.1 IASI

Developed by CNES in collaboration with EUMETSAT, the IASI instrument (Chalon et al., 2001; http://smsc.cnes.fr/IASI), onboard the MetOp-A polar platform, is a Fourier Transform Spectrometer that measures Earth-emitted infrared radiation. Launched in October 2006 and operational since July 2007, it provides 8461 spectral channels, between 15.5 µm (645 cm^{-1}) and 3.63 µm (2755 cm^{-1}) with a spectral resolution of 0.50 cm^{-1} after apodisation, and a regular spectral sampling interval of 0.25 cm^{-1}. MetOp-A crosses the Equator at 9.30 p.m. on its ascending node. IASI provides a near global coverage twice a day at a spatial resolution of 12 km at nadir. The period covered by the present study ranges from July 2007 to December 2012.

The method used to derive dust characteristics from IASI observations is a three-step algorithm based on a "Look-Up-Table" (LUT) approach (Pierangelo et al., 2004, 2005; Peyridieu et al., 2010, 2013). The first step determines the atmospheric state observed; the second step determines simultaneously the 10 µm AOD and the aerosol layer mean altitude while the dust coarse mode effective radius is determined in the third step. It is worth pointing out that, measuring in the infrared, IASI is essentially sensitive to the dust coarse mode with sensitivity to the fine mode of about 10 % or less. The dust model used is the "Mineral Transported" (MITR) aerosol model from the "Optical Properties of Clouds and Aerosols" (OPAC) database (Koepke et al., 1997; Hess et al., 1998). The main microphysical parameters associated with this model are: a mono modal lognormal distribution with a mode radius = 0.5 µm (r_{modN}), standard deviation of the size distribution = 2.2, particle density = 2.6 $g\,cm^{-3}$. At 10 µm, the corresponding optical parameters are: mass extinction efficiency = 0.24 $m^2\,g^{-1}$, single scattering albedo = 0.48, asymmetry factor = 0.44. Look-Up-Tables of IASI simulated brightness temperatures are calculated using the forward coupled radiative transfer model 4A/OP-DISORT (Scott and Chédin, 1981; Stamnes et al., 1988; http://4aop.noveltis.com). Entries to the model include: AOD, altitude, surface pressure, surface temperature and emissivity, viewing angle, and a set of about 600 atmospheric situations representative of the tropical band (30° S–30° N). Over land, surface spectral emissivity is taken from Capelle et al. (2012). IASI observations are processed spot by spot (daily), gridded 1° by 1°, and finally averaged monthly. Several aspects of the retrieval algorithm such as the robustness to aerosol model (size distribution, shape, and refractive index), the possible contamination by other aerosol species, the radiative transfer model bias removal, or the cloud mask including discrimination between clouds and aerosols, etc., were investigated in Pierangelo et al. (2004) and in Peyridieu et al. (2010).

2.2 AERONET

Accurate ground-based measurements are essential to evaluate satellite-derived aerosol characteristics. Here, we use the measurements routinely made and distributed by the Aerosol RObotic NETwork of sun-photometers (AERONET, Holben et al., 1998), particularly the Spectral Deconvolution Algorithm (SDA) retrieval of the coarse mode AOD monthly averages. Indeed, as explained by O'Neill (2003), the recognition that the aerosol particle size distribution is effectively bimodal permits the extraction of the fine and coarse mode optical depths from the spectral shape of the total aerosol optical depth. Comparison between infrared space borne and visible ground based instruments requires keeping in mind that IASI observations used here are made nighttime at 9.30 p.m. LT, when AERONET measures daytime; this difference should not be too important at monthly scale, except in the presence of a strong, recurrent, local diurnal cycle affecting the free troposphere to which IASI is most sensitive. A total of 38 AERONET sites have been selected within the tropical belt, both over sea and over land. Four coastal sites are used both over land and sea which means that AERONET measurements are associated with IASI data either over sea or over land. This selection takes into account the availability of a sufficient number of items throughout the time period studied: from July 2007 to December 2012, a maximum of 66 items may be expected; a few sites, representative of a region of interest, with less than 12 items

ACPD
13, 30143–30186, 2013

(6 sites over sea and 1 over land) have however been kept. To elaborate a sufficiently large and representative list of sites, the coarse mode AERONET AOD is of quality "Level 1.5" for a minority of sites (15) selected, meaning that they have been cloud-screened but may not have final calibration applied, all the other being of quality "Level 2.0" (quality-assured). Table 1 lists the 38 AERONET sites: name, longitude, latitude, 3-letter code, elevation (in m), 500 nm coarse mode AERONET AOD data quality level. Figure 1 shows the location of each AERONET site selected for this study: top for whole tropical belt, and, bottom, zoom on the Arabian Peninsula for the sake of readability. Out of all the sites listed in Table 1, the 9 first sites are located in the Persian Gulf or in the Arabian Peninsula, the following 9 are over Africa, the following 8 over the Atlantic Ocean, and the following 11 over Asia; the last site is located over Australia.

2.3 CALIOP

Launched in April 2006, the satellite CALIPSO with the on board two-wavelength depolarization lidar CALIOP permits an accurate determination of the aerosol altitude (Winker et al., 2009, 2010) to which IASI-derived altitude is here compared. CALIOP, a near-nadir viewing instrument, has a very narrow swath (beam diameter of 70 m at the Earth's surface, giving a 16 days repetition cycle). For that reason, starting from the L2 5 km aerosol layer product (version 3), monthly mean CALIOP altitudes are calculated at a resolution of $3^{\circ} \times 3^{\circ}$ following the approach and quality criteria of Tsamalis et al. (2013). It is worth recalling that the altitudes seen by either IASI or by CALIOP do not correspond to the same definition. For IASI, it is an "infrared-equivalent" altitude, i.e. the altitude at which half of the dust optical depth is below and half of the optical depth is above, when, for CALIOP, it is the mean value calculated from the vertical distribution of dust occurrence frequency (see Tsamalis et al., 2013 for details), thus independent from the dust load. The CALIOP mean altitude is calculated in this way in order to avoid the critical influence of the lidar ratio on the estimation of the extinction coefficient (and the optical depth), which might impact a mean altitude estimation

ACPD
13, 30143–30186, 2013

weighted by the dust load. Moreover, IASI shows low sensitivity to a complex layering of the dust (Pierangelo et al., 2004).

3 Method

IASI monthly mean $1^\circ \times 1^\circ$ gridded AOD and altitude are first averaged over boxes centered around each AERONET site. A large majority of the boxes ($\sim 70\,\%$) are of size $\pm 1.5^\circ$ by $\pm 1.5^\circ$. Over land, in particular, this standard box size may slightly vary according the characteristics of the terrain (presence of high relief, of lakes, of a complex coastal configuration, etc.). For each site, a month of the period studied for which IASI AOD and AERONET AOD data are both available enters the AOD evaluation procedure; the same rule applies for IASI altitude and CALIOP altitude. In the following such a couple of data will be referred to as one item.

To quantify how accurately IASI agrees with AERONET or CALIOP use is made here of a Taylor diagram approach (Taylor, 2001). As explained by the author, this diagram can concisely summarize how well two patterns match each other in terms of their correlation, their root-mean-square (RMS) difference, and the ratio of their variances. Here, the two patterns are IASI (AOD or altitude) on the one hand, AERONET for the AOD or CALIOP for the altitude, on the other. On this diagram the correlation coefficient and the RMS difference between the two fields, along with the ratio of the standard deviations of the two patterns, are all indicated by a single point on a two dimensional plot. In the following, we use the "normalized" version of the Taylor diagram, which means that the RMS difference and the two standard deviations have been normalized by the standard deviation of the corresponding reference field, here AERONET for the AOD or CALIOP for the altitude.

Moreover, because the diagram has been designed to convey information about centered pattern differences, we also use box and whiskers plots to characterize the distributions of the differences between the two patterns considered. This approach is important in the sense that such box plots display differences between populations without

ACPD
13, 30143–30186, 2013

making any assumptions of the underlying statistical distribution. In the plots presented here are shown the 1st and 3rd quartiles, the median, the ends of the whiskers being the minimum and maximum of all of the data remaining after elimination of “outliers” (see below).

For the AOD, such a comparison raises the problem of the difference between the two spectral domains used: infrared (IASI) and visible (AERONET). Assuming a mono modal size distribution in the two cases (sensitivity of IASI AOD to the fine mode is ∼ 10 % or less, Pierangelo, 2013), the IR/Vis ratio essentially depends on the width of the size distribution and on the effective radius. Because these parameters vary from one site to another, there is no one common factor reconciling the two observation metrics. To overcome this difficulty, a fit is done, site by site, including all the available items (monthly IASI-AERONET bins) over the period studied, resulting in an IR 10 µm AOD/500 nm coarse mode AERONET AOD “site ratio”. At this stage, it is important to point out that the quality of the fit depends on the number of items available (as said above, a maximum of 66 items may be expected). Averaged over all the sites, the mean ratio comes to 0.60 ± 0.17 for the sites over sea and 0.55 ± 0.16 for the sites over land. This statistics excludes sites with less than 10 items (7 sites), sites with an altitude greater than 1000 m (2 sites, see Table 1) and the two Tenerife sites (TEL and TES) due to their resulting much larger ratios (∼ 1.3; keeping these two sites increases the mean ratio to 0.69 ± 0.28). Kalashnikova and Kahn (2008) had already observed the particular behavior of these sites, still not clearly understood. Theoretical ratio can be estimated using a Lorenz-Mie calculation (Mishchenko et al., 2002 and http://ftp.giss.nasa.gov/pub/crmim/spher.f), the refractive indices of the MITR aerosol model and a monomodal lognormal size distribution. Figure 2 shows how the ratio varies with these variables, decreasing with the effective radius and increasing with the width of the distribution. For typical values of these variables from AERONET, the ratio IR at 10 µm/Vis coarse mode at 500 nm is expected to lie between 0.65 and 0.9. This is in reasonable agreement with the above observed values considering uncertainties on the variables entering the theoretical computation. This is also in reasonable agreement with values from Highwood et al. (2003). In the remaining of the paper, for each AERONET site, the visible AOD is multiplied by its site ratio prior to being compared to IASI infrared AOD.

Finally, all statistical results are given after having eliminated so-called "outliers" for which the difference between the IASI and the reference data stands too far from the mean of all the sites. Here, the test distance has been chosen so that about 7 % of the items are eliminated. Outliers may correspond to remaining thin clouds not detected by the cloud detection algorithm, to strong temporal aerosol heterogeneities (having in mind that IASI and AERONET do not often measure the same days in the month), or to limits of the IASI retrieval algorithm, or to errors in the AERONET (AOD) or CALIOP (altitude) observations.

4 Results

A few preliminary remarks are necessary to a better understanding of the following analysis. First, the signal induced on IASI observations by each variable of interest, here AOD or altitude, depends on the intensity of the variable. For example, the larger the AOD, the larger the signal, and a weak AOD is expected to be associated with a larger retrieval error. This is less trivial for the altitude but, generally, the higher the altitude the larger the signal. This is due to the decreasing thermal contrast between the surface and the atmosphere when approaching the surface. For that reason, infrared sounders show a limited sensitivity to the boundary layer. Second, the signal induced by altitude is intrinsically smaller than that induced by AOD: retrieving accurate altitude is more difficult, even more for low AOD. Third, the signal has to compete with the radiometric noise of the instrument: the larger the noise, the noisier the retrieved variable. IASI, a remarkably accurate and stable instrument, has a drawback with the larger noise of its short wavelength channels used for a good disentangling of the AOD and altitude signals; this difficulty has more impact on the altitude than on the AOD.

ACPD
13, 30143–30186, 2013

These remarks should help bringing the following results in the context of infrared remote sensing of aerosols.

4.1 Evaluation of IASI 10 µm AOD

In the following, for the sake of a simpler identification, each site name is followed by a parenthesized number referring either to Table 2 for sites over sea, or to Table 3 for sites over land. As mentioned previously, a few sites are used both over sea and over land which means that AERONET measurements are associated with IASI data either over sea or over land. This is the case of: Dakar, Karachi, Pune, and Solar_Village, the latter, an obvious land site, for reasons discussed below.

4.1.1 Evaluation of IASI 10 µm AOD over sea

Table 2 gives, site by site, the correlation (last column) obtained between IASI and 500 nm coarse mode AERONET AOD. For each site, identified by its full name, 3-digit code and number (resp., columns 1 to 3), the number of items in the statistics is also given. The last line of this table gives the overall statistics. Sites marked by an asterisk indicate that the AERONET coarse mode AOD at this site is "Level 1.5" instead of "Level 2.0" (see Sect. 2.2). Italicized names correspond to sites for which the full period averaged IASI AOD is less than 0.08, knowing that a majority of sites have an averaged AOD of the order of 0.15 (see also the AOD time series in the Supplement). With a total of 713 items and an overall correlation of 0.88, one may reasonably conclude that IASI matches well AERONET. Site by site, disparities appear with, for example, KAUST_Campus(7) and a stronger than the mean correlation of 0.96, not significant due to its only 5 items, or with CRPSM_Malindi(8) and a weaker correlation of 0.49, mainly due to the small IASI AOD observed throughout the period, at or even under the limit of the method (average AOD of 0.04), perhaps also due to the quality "Level 1.5" of this site. However, other "Level 1.5" sites show good correlations

ACPD
13, 30143–30186, 2013

as Pune(20) or Dhaka_University(21). Suppressing the elimination of outliers leads to an overall correlation of 0.80 for 770 items.

Figure 3 shows the Taylor diagram (normalized by the reference AERONET) for the IASI and the AERONET coarse mode AOD. On this figure, the labels (numbers) correspond to that of Table 2 and the symbol “av” stands for the result obtained when all items from the 25 sites over sea are merged. In addition to the good overall correlation of 0.88 already seen, this diagram brings into evidence an overall (“av”) normalized standard deviation similar to that of AERONET, marked by the cyan circle of radius 1 (by definition of the reference). In the following, the normalized standard deviation will be referred to as “amplitude”, as often representative of the amplitude of the seasonal cycle. CRPSM Malindi(8), with a weak correlation, shows a much larger amplitude (by about 30 %) compared to the reference. KAUST_Campus(7) with a strong correlation, and GOT_Seaprism(22) with a medium correlation, have similar large amplitudes but are not really significant due to their low numbers of items; see Table 2. Three sites of the Persian Gulf (Dhabi(2), Dhanah(3), Mussafa(5)) and Dakar(12) show smaller amplitudes (by about 25 %). For Dhabi(2) and Mussafa(5) to a lesser extent, the number of items is low. These differences in amplitude may, at least partially, be due to a difference in the phasing of the two products; this is, for example, the case of Dakar(12): see Sect. 4.4 and the AOD time series in Fig. S1 of the Supplement. They may also be due to the way the AERONET metrics is adapted to the IASI metrics (see Sect. 3) through a fit on all the items available for the site considered. As already explained in Sect. 3, too few AERONET measurements, poorly distributed throughout the time period studied, can render the fit not fully representative of the whole seasonal cycle. For some other sites, if the amplitude is that expected, the correlation is weaker and, as a consequence, the RMS larger. Among these, the weakest are MCO-Hanimaadhoo(19) and EPA-NCU(23). Both sites share being under the influence of a variety of aerosol sources as revealed by trajectory analysis (Eck et al., 2001; Wang et al., 2010). They are also sites in this list where conditions make the MITR aerosol model inappropriate; this problem is discussed in Sect. 4.3.

Figure 4 shows the box and whiskers plot for the difference between IASI and AERONET AOD: 1st, 3rd quartiles and median. The ends of the whiskers are the minima and maxima of all of the data, outliers excluded. For the overall sample, there is almost no skewness, and a relatively small inner quartile range (3rd quartile minus 1st quartile) of ∼ 0.05. Most sites show a small skewness with the noticeable exception of Izana(14), but the altitude of this site is of ∼ 2400 m (see also Sect. 3), and of the sites with too small numbers of items (Dhabi(2), KAUST_Campus(7), Dhaka_University(21), etc.) which actually display dubious results as far as the data distribution is concerned.

4.1.2 Evaluation of IASI 10 µm AOD over land

As in Table 2 for the sites over sea, Table 3 gives the correlation (last column) obtained between IASI and 500 nm coarse mode AERONET AOD for the sites over land. Here, the overall correlation reaches 0.74 for 582 items (0.67 for 621 items without elimination of the outliers), a relatively good result keeping in mind that, here, the proportion of "Level 1.5" sites is larger than over sea. As for sites over sea, site by site disparities appear with, for example, the high correlation (0.87) of Tamanrasset_IMN(8) however with only 14 items available, or the weak correlation (0.48) of Solar_Village(2). This poor correlation for a site with a relatively high number of items (55) has at least two explanations: terrain heterogeneities and elevation (about 850 m). This situation complicates the retrieval of AOD by rendering channels sounding low in the atmosphere even more transparent and hence more affected by surface heterogeneities. As a consequence, errors in the surface emissivity and/or temperature have larger consequences. This has led us to associate Solar_Village AERONET measurements with IASI data at the nearest region (centred at 27° N, 51° E, box of ±1° in latitude and longitude) over sea of the Persian Gulf, having in mind the prevalence of roughly similar weather conditions over the Arabian Peninsula during the pre-monsoonal (spring) and monsoonal (summer) period, when maximum dust activity occurs (Walters Sr. and Sjoberg, 1990; Smirnov et al., 2002; Leon and Legrand, 2003). This time, a strong correlation of 0.83 is obtained as seen in Table 2 and Fig. 3. We see this result as a confirmation of the

ACPD
13, 30143–30186, 2013

increased difficulty in retrieving aerosol characteristics over "difficult" terrains. Except Zouerate-Fennec(10) with a correlation of 0.76, all other "Level 1.5" sites show relatively weak correlations.

Figure 5 shows the Taylor diagram (normalized by the reference AERONET) for IASI and AERONET coarse mode AOD. The largest discrepancies, marked by a much too low amplitude compared to AERONET, can be seen at three "Level 1.5" sites (Hada_el_Sham(3), Zinder_Airport(9), and Zouerate_Fennec (10)) although the latter shows a strong correlation, but Pune(13), also a "Level 1.5" site, shows amongst the best agreement. Among the "Level 2" sites, Tamanrasset_IMN(8) shows a strong correlation but too low an amplitude (~ 0.75), Gual_Pahari(15) has good results, and Solar_Village(2) has the weakest correlation and an amplitude too low by $\sim 20\,\%$ (note that, as an "over sea" site, its amplitude is almost equal to 1; see Fig. 3). The amplitude corresponding to the whole ensemble of items from the 17 sites over land merged ("av" on the graph) is slightly smaller than that of the reference (by 13 %). Actually, this is a general result: all sites show a deficit, some of them (Mezaira(1), Karachi(12), Jaipur(14)) more than the others. This is all the more true over Sahara, most sites being "Level 1.5". These results confirm that the presence of pronounced terrain heterogeneities has a negative impact on the accuracy of the AOD retrieved from IASI. This is due to the increased difficulty in determining surface characteristics (emissivity and temperature; see Capelle et al., 2012).

Figure 6 shows the box and whiskers plot for the difference between IASI and AERONET AOD: 1st, 3rd quartiles and median for the sites over land. They are significantly worse than over sea with a majority of skewed distributions, most pronounced for Mezaira(1) and Tamanrasset_IMN(8), the latter with only 14 items. As a consequence, the overall distribution is slightly skewed and the ends of the whiskers are at about ± 0.15 instead of ± 0.1 over sea.

Both over sea (coastal) and over land, the sites of the Middle East are not among the best with a few exceptions. This might be due to the aerosol heterogeneity in this region (Kaskaoutis et al., 2010) where coarse mode desert dust aerosols often mix with fine mode pollution aerosols largely produced by the petroleum industry, themselves possibly affected by aerosol humidification growth (Smirnov et al., 2002; Eck et al., 2008; Reid et al., 2005–2008; Basart et al., 2009). This is somewhat similar for Ilorin(11) and Kanpur(16) (Singh et al., 2004; Eck et al., 2010). One may remark that the "Global dust model intercomparison in AeroCom Phase I" (Huneeus et al., 2011) came to similar conclusions for the Middle East AERONET stations and the coarse mode AOD. More generally, results over land are significantly worse than over sea, mainly due to the greater complexity of the surface (heterogeneities, elevation) and to the episodic presence of dust in the lower troposphere, particularly for sites close to active sources (Sahara, for example), to which IASI is poorly sensitive contrary to AERONET. Close to the sources, the measurement time difference between IASI (at night) and AERONET may also be a problem.

4.2 Evaluation of IASI altitude

Before presenting results of the comparison between IASI and CALIOP, it is worth pointing out that comparing two samples of satellite data provides more items than comparing one sample of satellite data to AERONET ground based data. Over sea, for example, if the total number of items obtained is not that larger (925 instead of 713 for the AOD), all sites but two appear to have at least 20 items; exceptions are for Ningbo(24) with 12 items and Lucinda(25) with 15 items. As in Table 2 for the AOD, Table 4 gives the correlation (last column) obtained between IASI and CALIOP altitude over sea. With a correlation of 0.78 based upon 925 items, we infer that IASI matches CALIOP satisfactorily. The slightly weaker correlation than for AOD had to be expected due to, (i) the different definitions of the two altitude products, (ii) the large differences in the space-time resolution of IASI and CALIOP, (iii) the sensitivity of IASI, lower to altitude than to AOD (Pierangelo et al., 2004). Here again, site by site disparities appear with, for example, sites far from the sources characterized by a weak AOD (see Table 2) throughout the time period. CRPSM_Malindi(8), Camaguey(10), La_Parguera(16), Ragged_Point(17), EPA-NCU(23), or Lucinda(25), are examples of such sites. This is due to the fact that a low AOD increases the difficulty of determining the altitude from IASI (there are a few exceptions: MCO-Hanimaadhoo(19) or Pune(20), which show strong correlations of 0.80 and 0.79, resp.).

Figure 7, similarly to Fig. 3 for the AOD, shows the Taylor diagram for IASI and CALIOP altitude over sea, CALIOP being the reference. In addition to the good overall correlation of 0.78 already seen, if this diagram shows overall amplitude similar to that of CALIOP, it also brings into evidence a large dispersion of the amplitudes for the sites. Too large for sites like Dhabi(2), Dhadnah(3) or Dakar(12), and too small for the three sites indicated as Tenerife(13–15), overlapping with an amplitude of ~ 0.75 and a correlation of ~ 0.70. Among the "Level 2" sites, the weakest correlation, 0.52, is that of EPA-NCU(23). The box and whiskers plot for the difference between IASI and CALIOP altitude, 1st, 3rd quartiles and median, over sea is shown in Fig. 8. For the overall sample, there is no skewness and a relatively small inner quartile range (3rd quartile minus 1st quartile) of ~ 0.55 km. Most sites show a small skewness with the exception of CRPSM_Malindi(8), 0.14 km, Camaguey(10), 0.10 km, Dakar(12), −0.17 km, and GOT_Seaprism(22), −0.21 km. Lucinda(25) again shows a strange behavior. Inner quartile range vary from about 0.36 km for Kaust_Campus(7) to about 0.8 km for Abu_Al_Bukhoosk(1).

For a majority of sites over land, essentially over deserts, results for altitude are not satisfactory. In addition to the reasons discussed above for the AOD, we must mention the smaller signal induced by the altitude compared to the one induced by the AOD. Work is in progress to solve these difficulties.

4.3 Impact of the refractive index in the infrared

If numerous measurements of the aerosol refractive indices actually exist in the visible part of the spectrum, this is not the case in the infrared. However, refractive indices in the infrared are often marked by a relatively large spectral variability from one source of aerosol to another. Sokolik et al. (1998), listing most of the existing measurements of mineral aerosol infrared refractive indices, well illustrate this variability. This can cause important changes in the aerosol optical characteristics (Sokolik et al., 1998; Claquin et al., 1998; Sokolik and Toon, 1999; Pierangelo, 2013) and, consequently, in the dust radiative forcing, both in the infrared and in the visible. Figure 9 shows infrared refractive indices from three sources: "MITR" from the OPAC data base (Hess et al., 1998), resulting from the measurements by Volz (1973) and representative of desert dust far from the sources; "dust-like" from the measurements by Volz (1972, 1973), more representative of non desert mineral aerosols generated from soil; "Revisited" IR refractive indices were proposed by Balkanski et al. (2007) in an effort to reevaluate mineral aerosol radiative forcings. At this stage, it is worth pointing out that, in the infrared, the impact of the refractive index is difficult to quantify a priori since it depends on both its imaginary and real parts at the central wavelengths of *all* the channels used in the retrieval process (Pierangelo et al., 2004). Locations of the IASI channels used in the present approach are shown on Fig. 9 by the vertical bars.

Because this study was carried out using a single refractive index model, actually the MITR model (Hess et al., 1998; see Sect. 2.1) whatever the location of the site considered is, it appeared important to test the sensitivity of the results to a change of the refractive index. IASI results have thus been reevaluated using the Balkanski et al. (2007) mineral dust refractive index which shows significant differences with the "MITR" model, in particular around 9.3, 11.5 or 11.8 µm, as illustrated by Fig. 9.

With this new assumption, new LUTs have been computed and the whole retrieval process redone. Figure 10 summarizes the differences found between the "MITR evaluation" and this new evaluation for the sites over land (see Table 3). On this figure are shown differences, site by site and total, between "MITR" and "Revisited" for the correlation (red) and the amplitude (normalized standard deviation; blue) for the AOD (IASI vs. AERONET). Positive (resp. negative) values mean better correlation and amplitude closer to 1 (amplitude of the AERONET reference) for "MITR" (resp. "Revisited"). A few conclusions stand out from this comparison. Concerning the correlation, there are four differences larger than 0.10. Two are in favour of "MITR": Dakar(6) by 0.12 and Gual_Pahari(15) by 0.15, the latter with too low a number of items to be re-

Discussion Paper | Discussion Paper | Discussion Paper | Discussion Paper |

ACPD
13, 30143–30186, 2013

Evaluation of IASI derived dust aerosols characteristics

V. Capelle et al.

ally significant; two are in favour of the "Revisited" IR refractive indices: Ilorin(11) by 0.11 and Kanpur(16) by 0.17, a site being under the influence of the Thar desert, the primary potential source of dusts in the Indian subcontinent (Dey et al., 2004 and references herein). Differences in amplitude are more contrasted with three sites in favour of "MITR" (Mezaira(1), Solar_Village(2), and Ilorin(11)), and four sites in favour of "Revisited" (DMN_Maine_Soroa(7), Karachi(12), Pune(13), and Kanpur(16)). Some sites show larger correlation but smaller amplitude contrary, for example, to Kanpur with the two results in favour of "Revisited". Concerning the box and whiskers results we have observed that differences in the median are negligible and that differences in the inner quartile range are slightly more important, the three largest differences (however less than 0.04) being in favour of "Revisited".

These results bring into evidence: (i), the significant impact of this change in refractive index model for some sites; (ii), the relevance of the Sokolik et al. (1998) recommendation regarding the use of such or such refractive index according to the geographical region considered, (iii), the relative robustness of the IASI retrievals to the refractive index for sites marked by a strong prevalence of desert dust influence with, however, a few marked exceptions. Differences between the two experiments made here are significant and point out the need of more new experimental measurements.

4.4 AOD and altitude time series

Time series of the AOD from IASI and AERONET and of the altitude from IASI and CALIOP give another view of the degree of agreement between the different sources of products. They also highlight the frequent lack of AERONET data throughout the period of study. Holes are also seen for IASI due to not enough IASI daily results in the monthly average (presence of persistent clouds, rejection by the algorithm, etc.). Because of the relatively large number of sites considered in this study, we present the time series figures in the "Supplement" associated with this paper. Figure S1 shows time series of the 10 µm IASI AOD (red), and of the AERONET coarse mode 500 nm AOD (black), for the sites over sea. AERONET AOD is scaled by the IR/Vis ratio determined as explained in Sect. 3 and shown top-left of each figure. Figure S2 shows similar time series for the sites over land. Several remarks can be made about these figures: (i), a relatively modest result seen from the Taylor diagrams may be explained by a small shift of the IASI time series with respect to AERONET; this is, for example, the case for Dhadna(3), Mussafa(5) or Dakar(12). It can also result from the smallness of the AOD (CRPSM_Malindi(8)). A good correlation may mask an IR/Vis ratio a priori far from its theoretical value (Izana(14), which site elevation (2400 m) is however questionable). For the same site, the difference between the amplitudes of the IASI and the AERONET time series is obvious. Similar remarks can be made for the sites over land. For example, the quite large amplitudes of the AERONET time series for Mezaira(1), Agoufou(4), Banizoumbou(5), DMN_Maine_Soroa(7), Zinder_Airport(9), or Zouerate_Fennec(10), all "Level 1.5" sites, except the first one. The same time series also bring into evidence the likely too high IASI AOD outside the aerosol season. Incidentally, the largest IASI AOD ever observed in this study, ~ 0.7, is for Qiandaohu(17) over land. There are no AERONET measurements for this event (December 2008) but one exists for the nearby site of LA_TM (119.40° E, 30.32° N). Figure S3 shows the corresponding AOD time series which confirm the IASI observation for this event. Figure S4 shows time series of the IASI (red) and CALIOP (green) altitude (km) for the sites over sea. The most obvious remark is the (expected) difficulty of deriving altitude in case of weak AOD (see, for example, CRPSM_Malindi(8), or EPA_NCU(23)). Also, there are several amplitude (Tenerife sites (13–15), Karachi(18), etc.) or shift (Calhau(9), Capo_Verde(11), etc.) problems, illustrating that improving the method is still necessary.

5 Discussion and conclusions

5.1 AOD

In this study, IASI-derived dust AOD has been evaluated using AERONET ground-based measurements of the 500 nm coarse mode AOD for 38 sites (among which four

ACPD
13, 30143–30186, 2013

are used both over sea and land) of the tropical band. There are sites over sea, over land, and over desert. Most sites are of AERONET quality "Level 2" (quality-assured), the rest being of quality "Level 1.5", meaning that they have been cloud-screened but may not have final calibration applied. The method relies on the analysis of Taylor diagrams and of box and whiskers plots. To overcome the difficulty raised by the difference between the two spectral domains used to derive the AOD, hence having different metrics, a fit is done, site by site, including all the available items for the period studied, resulting in an IR 10 µm IASI AOD/500 nm coarse mode AERONET AOD "site ratio". Theory shows that this ratio essentially depends on the width of the size distribution and on the effective radius. These parameters varying from one site to another (and, often, from one day to the next), there is no one common factor reconciling the two observation metrics. For sites over sea, we infer a mean ratio of 0.60 ± 0.17 in relatively good agreement with already published values (Highwood et al., 2003); slightly lower results are obtained over land: 0.55 ± 0.16. The dispersion is significant and comes not only from the variability, site by site, of the influencing variables, but also from the possible improper use of the "MITR" aerosol model for such or such site. If too few items are available over the time period studied, the fit may not be really representative of the whole seasonal cycle and hence may lead to an improper ratio: the smaller the number of items, the less reliable the results. In general, results are significantly better over sea than over land, this being essentially due to a better knowledge of the surface characteristics, particularly for heterogeneous terrains.

Over sea, the main results found for the AOD in this work are: (i), a strong overall correlation of 0.88 between IASI and AERONET monthly mean AOD for the 713 items representing all the months available at the 25 sites; (ii), weaker correlations observed for some sites with complex aerosol situations marked by the influence of a variety of sources, or for some sites that may reasonably be suspected not to correspond to the "MITR" model used here (Hess et al., 1998); an overall amplitude (normalized standard deviation) similar to that of AERONET; (iii) no skewness of the overall sample (as well as of most site samples) and a relatively small inner quartile range of ~ 0.05.

ACPD
13, 30143–30186, 2013

Over land, the overall correlation comes to 0.74 for the 582 items representing all the months available at the 17 sites over. This is a relatively high correlation keeping in mind that, here, the proportion of "Level 1.5" sites is larger than over sea. All sites show smaller amplitude than that of the reference AERONET (by ~ 13 % for the overall sample), the stronger discrepancy found over Sahara, where most sites are "Level 1.5". In addition to the explanations already seen for sites over sea, pronounced terrain heterogeneities, increasing the difficulty of determining surface characteristics (emissivity and temperature; see Capelle et al., 2012), have a negative impact on the AOD accuracy. The box and whiskers results (Fig. 5) are significantly degraded compared to the ones over sea with a majority of skewed distributions.

5.2 Altitude

With 925 items for the whole period and all sites over sea and overall correlation of 0.78, it can be concluded that IASI matches CALIOP satisfactorily. A correlation weaker than for the AOD was expected due the great difference between the two approaches (definition of the altitude, differences in the space-time resolutions, lower sensitivity of IASI to altitude than to AOD). It is also seen that low IASI AODs increase the difficulty of determining the altitude from IASI. The Taylor diagram for the altitude over sea (Fig. 7) shows overall amplitude similar to that of AERONET, and also brings into evidence a large dispersion in the site amplitudes. The box and whiskers plot (Fig. 8) for the overall sample shows a small skewness and a relatively small inner quartile range (3rd quartile minus 1st quartile) of ~ 0.55 km. Most sites show no pronounced skewness. Results over land, particularly over deserts, are not satisfactory. We suggest that this is due to terrain heterogeneities and elevation as well as to the residual presence of dust aerosols in the lower troposphere. Work is in progress to solve these difficulties.

5.3 Problem of the refractive index

One of the potential weaknesses of the present evaluation is the systematic use of the "MITR" refractive index model. The experiment consisting in changing this model with the "Revisited" IR refractive indices from Balkanski et al. (2007) and proceeding to a new evaluation has brought some indications concerning the sensitivity of such an evaluation to this assumption. First, the significant impact of this change in refractive index model for some sites; second, the relevance of the Sokolik et al. (1998) recommendations regarding the use of refractive index adapted to the geographical region considered; third, the relative robustness of the IASI retrievals to the refractive index for sites marked by a strong prevalence of desert dust influence. This highlights the need of more new experimental measurements of refractive indices for more geographical aerosol source regions. The method used here to derive aerosol characteristics from IASI is immediately applicable to such new measurements.

5.4 Difficulties of the evaluation

Such an evaluation meets several problems. First, the number of IASI-AERONET monthly mean AOD bins per site is never equal to the number of months of the period studied (66). The most complete site is, by far, Capo_Verde, with 62 items. The overall mean is ~ 31 and the time distribution is not always representative of the seasonal cycle. Second, measuring either in the visible or in the infrared, AERONET and IASI do not share the same AOD metrics. The fit used to adapt the AERONET metrics to that of IASI must be made site by site because of the dependence of the infrared to visible ratio on (essentially) the size distribution and the effective radius, themselves varying from one site to another. A wrong ratio may result from a fit with too small a number of items. It may also result from the improper use of the "MITR" model for such or such site. Third, over land and particularly over desert, terrain heterogeneities may render the determination of the surface characteristics more problematic, resulting in a degradation of the dust properties derived from IASI. Moreover, the episodic presence of

ACPD
13, 30143–30186, 2013

dust within the lower troposphere, particularly for sites close to active sources (Sahara, for example), to which IASI is poorly sensitive, contrary to AERONET, may also lead to differences between ground based AERONET observations and IASI retrievals. Finally, the large increase of the radiometric noise of short wavelengths IASI channels hampers the altitude retrieval which quality relies on a combination of longwave and shortwave channels (Pierangelo et al., 2004; Peyridieu et al., 2013).

In spite of these difficulties, the overall agreement between IASI and AERONET for the AOD and between IASI and CALIOP for the altitude is satisfactory. AERONET, CALIOP, and IASI, all have their advantages and drawbacks: the present results demonstrate the usefulness of IASI data as an additional constraint to a better knowledge of the impact of aerosols on the climate system.

Supplementary material related to this article is available online at http://www.atmos-chem-phys-discuss.net/13/30143/2013/acpd-13-30143-2013-supplement.pdf.

Acknowledgements. We thank the PI investigators and their staff for establishing and maintaining the AERONET sites used in this investigation. We are also happy to thank the ICARE Thematic Center for providing us with CALIPSO/CALIOP data (http://www.icare.univ-lille1.fr/). This work has been supported in part by the European Community under the Grant Agreement no. 283576 (MACC project) and by CNRS, CNES and Ecole Polytechnique. We have also benefited from the large facilities of IDRIS, the computer center of CNRS. Thanks are also due to Y. Balkanski for providing us with revisited infrared dust refractive indices.

The publication of this article is financed by CNRS-INSU.

References

Balkanski, Y., Schulz, M., Claquin, T., and Guibert, S.: Reevaluation of Mineral aerosol radiative forcings suggests a better agreement with satellite and AERONET data, Atmos. Chem. Phys., 7, 81–95, doi:10.5194/acp-7-81-2007, 2007.

Basart, S., Pérez, C., Cuevas, E., Baldasano, J. M., and Gobbi, G. P.: Aerosol characterization in Northern Africa, Northeastern Atlantic, Mediterranean Basin and Middle East from direct-sun AERONET observations, Atmos. Chem. Phys., 9, 8265–8282, doi:10.5194/acp-9-8265-2009, 2009.

Capelle, V., Chédin, A., Péquignot, E.,Schlüssel, P., Newman, S. M., and Scott, N. A.: Infrared continental surface emissivity spectra and skin temperature retrieved from IASI observations over the tropics, J. Appl. Meteor. Climatol., 51, 1164–1179, doi:10.1175/JAMC-D-11-0145.1, 2012.

Chalon, G., Cayla, F., and Diebel, D.: IASI: An Advanced Sounder for Operational Meteorology, Proceedings of the 52nd Congress of IAF, Toulouse France, October 2001, 2001.

Chiapello, I., Bergametti, G. G., Gomes, L., Chatenet, B., Dulac, F., Pimenta, J., and Santos Suares, E.: An additional low layer transport of Sahelian and Saharan dust over the North-Eastern Tropical Atlantic, Geophys. Res. Lett., 22, 3191–3194, 1995.

Chiapello, I., Moulin, C., and Prospero, J. M.: Understanding the long-term variability of African dust transport across the Atlantic as recorded in both Barbados surface concentrations and large-scale Total Ozone Mapping Spectrometer (TOMS) optical thickness, J. Geophys. Res., 110, D18S10, doi:10.1029/2004JD005132, 2005.

Claquin, T., Schulz, M., Balkanski, Y., and Boucher, O.: Uncertainties in assessing radiative forcing by mineral dust, Tellus B, 50, 491–505, 1998.

De Souza-Machado, S., Strow, L. L., Motteler, H., and Hannon, S.: Infrared dust spectral signatures from AIRS, Geophys. Res. Lett., 33, L03801, doi:10.1029/2005GL024364, 2006.

Dey, S., Tripathi, S. N., Singh, R. P., and Holben, B. N.: Influence of dust storms on the aerosol optical properties over the Indo-Gangetic basin, J. Geophys. Res., 109, D20211, doi:10.1029/2004JD004924, 2004.

Eck, T. F., Holben, B. N., Dubovik, O., Smirnov, A., Slutsker, I., Lobert, J. M., and Ramanathan, V.: Column-integrated aerosol optical properties over the Maldives during the northeast monsoon for 1998–2000, J. Geophys. Res., 106, 28555–28566, 2001.

Eck, T. F., Holben, B. N., Reid, J. S., Sinyuk, A., Dubovik, O., Smimov, A., Giles, D., O'Neill, N. T.,Tsay, S.-C., Ji, Q., Al Mandoos, A., Ramzan Khan, M., Reid, E. A., Schafer, J. S., Sorokine, M., Newcomb, W., and Slutsker, I.: Spatial and temporal variability of column-integrated aerosol optical properties in the southern Arabian Gulf and United Arab Emirates in summer, J. Geophys. Res., 113, D01204, doi:10.1029/2007JD008944, 2008.

Eck, T. F., Holben, B. N., Sinyuk, A., Pinker, R. T., Goloub, P., Chen, H., Chatenet, B., Li, Z., Singh, R. P., Tripathi, S. N., Reid, J. S., Giles, D. M., Dubovik, O., O'Neill, N. T., Smirnov, A., Wang, P., and Xia, X.: Climatological aspects of the optical properties of fine/coarse mode aerosol mixtures, J. Geophys. Res., 115, D19205, doi:10.1029/2010JD014002, 2010.

Formenti, P., Schütz, L., Balkanski, Y., Desboeufs, K., Ebert, M., Kandler, K., Petzold, A., Scheuvens, D., Weinbruch, S., and Zhang, D.: Recent progress in understanding physical and chemical properties of African and Asian mineral dust, Atmos. Chem. Phys., 11, 8231–8256, doi:10.5194/acp-11-8231-2011, 2011.

Forster, P., Ramaswamy, V., Artaxo, P., Berntsen, T., Betts, R., Fahey, D. W., Haywood, J., Lean, J., Lowe, D. C., Myhre, G., Nganga, J., Prinn, R., Raga, G., Schulz, M., and Van Dorland, R.: Radiative forcing of climate change, in: Climate Change 2007: The Physical Science Basis. Contribution of Working Group I to the Fourth Assessment Report of the Intergovernmental Panel on Climate Change, edited by: Solomon, S., Qin, D., Manning, M., Chen, Z., Marquis, M., Averyt, K. B., Tignor, M., and Miller, H. L., Cambridge Univ. Press, Cambridge, UK and New York, NY, USA, 129–234, 2007.

Hansen, J., Sato, M., and Ruedy, R.: Radiative forcing and climate response, J. Geophys. Res., 102, 6831–6864, doi:10.1029/96JD03436, 1997.

Haywood, J. M. and Ramaswamy, V.: Global sensitivity studies of the direct radiative forcing due to anthropogenic sulfate and black carbon aerosols, J. Geophys. Res., 103, 6043–6058, doi:10.1029/97JD03426, 1998.

Hess, M., Koepke, P., and Schult, I.: Optical properties of aerosols and clouds: the software package OPAC, Bull. Am. Met. Soc., 79, 831–844, 1998.

Highwood, E., Haywood, J. M., Silverstone, M. D., Newman, S. M., and Taylor, J. P.: Radiative properties and direct effect of Saharan dust measured by the C-130 aircraft during Saharan Dust Experiment (SHADE), 2. Terrestrial spectrum, J. Geophys. Res., 108, 8578, doi:10.1029/2002JD002552, 2003.

Holben, B. N., Eck, T. F., Slutsker, I., Tanre, D., Buis, J. P., Setzer, A., Vermote, E., Reagan, J. A., Kaufman, Y. J., Nakajima, T., Lavenu, F., Jankowiak, I., and Smirnov, A.: AERONET – a feder-

ACPD
13, 30143–30186, 2013

Evaluation of IASI derived dust aerosols characteristics

V. Capelle et al.

ated instrument network and data archive for aerosol characterization, Rem. Sens. Environ., 66, 1–16, 1998.
Huneeus, N., Schulz, M., Balkanski, Y., Griesfeller, J., Prospero, J., Kinne, S., Bauer, S., Boucher, O., Chin, M., Dentener, F., Diehl, T., Easter, R., Fillmore, D., Ghan, S., Ginoux, P., Grini, A., Horowitz, L., Koch, D., Krol, M. C., Landing, W., Liu, X., Mahowald, N., Miller, R., Morcrette, J.-J., Myhre, G., Penner, J., Perlwitz, J., Stier, P., Takemura, T., and Zender, C. S.: Global dust model intercomparison in AeroCom phase I, Atmos. Chem. Phys., 11, 7781–7816, doi:10.5194/acp-11-7781-2011, 2011.
Kalashnikova, O. V. and Kahn, R. A.: Mineral dust plume evolution over the Atlantic from MISR and MODIS aerosol retrievals, J. Geophys. Res., 113, D24204, doi:10.1029/2008JD010083, 2008.
Kaskaoutis, D. G., Kalapureddy, M. C. R., Krishna Moorthy, K., Devara, P. C. S., Nastos, P. T., Kosmopoulos, P. G., and Kambezidis, H. D.: Heterogeneity in pre-monsoon aerosol types over the Arabian Sea deduced from ship-borne measurements of spectral AODs, Atmos. Chem. Phys., 10, 4893–4908, doi:10.5194/acp-10-4893-2010, 2010.
Kaufman, Y. J., Tanre, D., Gordon, H. R., Nakajima, T., Lenoble, J., Frouin, R., Grassl, H., Hermann, B. M., King, M. D., and Teillet, P. M.: Passive remote sensing of tropospheric aerosol and atmospheric correction for the aerosol effect, J. Geophys. Res., 102, 16815–16830, doi:10.1029/97JD01496, 1997.
Klüser, L., Martynenko, D., and Holzer-Popp, T.: Thermal infrared remote sensing of mineral dust over land and ocean: a spectral SVD based retrieval approach for IASI, Atmos. Meas. Tech., 4, 757–773, doi:10.5194/amt-4-757-2011, 2011.
Klüser, L., Kleiber, P., Holzer-Popp, T., Grassian, V. H.: Desert dust observation from space-Application of measured mineral component infrared extinction spectra, Atmos. Environ., 54, 419–427, 2012.
Knippertz, P. and Todd, M. C.: Mineral dust aerosols over the Sahara: Meteorological controls on emission and transport and implications for modeling, Rev. Geophys., 50, RG1007, doi:10.1029/2011RG000362, 2012.
Koepke, P., Hess, M., Schult, I., and Shettle, E. P.: Global aerosol data set, Rep. No. 243, Max-Planck Institut für Meteorologie, Hamburg, Germany, 44 pp., 1997.
Legrand, M, Bertrand, J. J., Desbois, M., Menenger, L., Fouquart, Y.: The potential of infrared satellite data for the retrieval of saharan-dust optical depth over Africa, J. Appl. Meteorol., 28, 309–319, doi:10.1175/1520-0450(1989), 1989.

Léon, J.-F. and Legrand, M.: Mineral dust sources in the surroundings of the north Indian Ocean, Geophys. Res. Lett., 30, 1309, doi:10.1029/2002GL016690, 2003.

Maher, B. A., Prospero, J. M., Mackie, D., Gaiero, D., Hesse, P. P., and Balkanski, Y.: Global connections between aeolian dust, climate and ocean biogeochemistry at the present day and at the last glacial maximum, Earth-Sci. Rev., 99, 61–97, doi:10.1016/j.earscirev.2009.12.001, 2010.

Mahowald, N. M., Kloster, S., Engelstaedter, S., Moore, J. K., Mukhopadhyay, S., McConnell, J. R., Albani, S., Doney, S. C., Bhattacharya, A., Curran, M. A. J., Flanner, M. G., Hoffman, F. M., Lawrence, D. M., Lindsay, K., Mayewski, P. A., Neff, J., Rothenberg, D., Thomas, E., Thornton, P. E., and Zender, C. S.: Observed 20th century desert dust variability: impact on climate and biogeochemistry, Atmos. Chem. Phys., 10, 10875–10893, doi:10.5194/acp-10-10875-2010, 2010.

Markowicz, K. M., Flatau, P. J., Vogelmann, A. M., Quinn, P. M., and Welton, E.: Influence of relative humidity on aerosol radiative forcing: an ACE-Asia experiment perspective. J. Geophys. Res., 108, 8662, doi:10.1029/2002JD003066, 2003.

Mishchenko, M. I., Travis, L. D., and Lacis, A. A.: Scattering, Absorption, and Emission of Light by Small Particles, Cambridge University Press, Cambridge, 2002.

Müller, D., Lee, K.-H., Gasteiger, J., Tesche, M., Weinzierl, B., Kandler, K., Müller, T., Toledano, C., Otto, S., Althausen, D., and Ansmann, A.: Comparison of optical and microphysical properties of pure Saharan mineral dust observed with AERONET Sun photometer, Raman lidar, and in situ instruments during SAMUM 2006, J. Geophys. Res., 117, D07211, doi:10.1029/2011JD016825, 2012.

Myhre, G. and Stordal, F.: Global sensitivity experiments of the radiative forcing due to mineral aerosols, J. Geophys. Res., 106, 18193–18204, 2001.

O'Neill, N. T., Eck, T. F., Smirnov, A., Holben, B. N., and Thulasiraman, S.: Spectral discrimination of coarse and fine mode optical depth, J. Geophys. Res., 108, 4559, doi:10.1029/2002JD002975, 2003.

Otto, S., de Reus, M., Trautmann, T., Thomas, A., Wendisch, M., and Borrmann, S.: Atmospheric radiative effects of an in situ measured Saharan dust plume and the role of large particles, Atmos. Chem. Phys., 7, 4887–4903, doi:10.5194/acp-7-4887-2007, 2007.

Peyridieu, S., Chédin, A., Tanré, D., Capelle, V., Pierangelo, C., Lamquin, N., and Armante, R.: Saharan dust infrared optical depth and altitude retrieved from AIRS: a focus over North

ACPD

13, 30143–30186, 2013

Atlantic – comparison to MODIS and CALIPSO, Atmos. Chem. Phys., 10, 1953–1967, doi:10.5194/acp-10-1953-2010, 2010.

Peyridieu, S., Chédin, A., Capelle, V., Tsamalis, C., Pierangelo, C., Armante, R., Crevoisier, C., Crépeau, L., Siméon, M., Ducos, F., and Scott, N. A.: Characterisation of dust aerosols in the infrared from IASI and comparison with PARASOL, MODIS, MISR, CALIOP, and AERONET observations, Atmos. Chem. Phys., 13, 6065–6082, doi:10.5194/acp-13-6065-2013, 2013.

Pierangelo, C.: Aerosol remote sensing, in: Springer-Praxis Books: Environmental Sciences, Lenoble, J., Remer, L., and Tanré, D., ch. 9, 223–282, 390 pp., ISBN-13: 9783642174407, 2013.

Pierangelo, C., Chédin, A., Heilliette, S., Jacquinet-Husson, N., and Armante, R.: Dust altitude and infrared optical depth from AIRS, Atmos. Chem. Phys., 4, 1813–1822, doi:10.5194/acp-4-1813-2004, 2004.

Pierangelo, C., Mishchenko, M., Balkanski, Y., and Chédin, A.: Retrieving the effective radius of Saharan dust coarse mode from AIRS, Geophys. Res. Lett., 32, L20813, doi:10.1029/2005GL023425, 2005.

Reid, J. S., Piketh, S. J. R., Kahn, R., Bruintjes, R. T., Holben, B. N.: A Summary of First Year Activities of the United Arab Emirates Unified Aerosol Experiment: UAE2, Naval Research Laboratory report nb. NRL/MR/7534–05-8899, 150 pp., 2005.

Reid, J. S., Piketh, S. J., Walker, A. L., Burger, R. P., Ross, K. E., Westphal, D. L., Bruintjes, R. T., Holben, B. N., Hsu, N. C., Jensen, T. L., Kahn, R. A., Kuciauskas, A. P., Al Mandoos, A., Al Mangoosh, A., Miller, S. D., Porter, J. N., Reid, E. A., and Tsay, S. C.: An overview of UAE2 flight operations: Observations of summertime atmospheric thermodynamic and aerosol profiles of the southern Arabian Gulf, J. Geophys. Res., 113, D14213, doi:10.1029/2007JD009435, 2008.

Ryder, C. L., Highwood, E. J., Rosenberg, P. D., Trembath, J., Brooke, J. K., Bart, M., Dean, A., Crosier, J., Dorsey, J., Brindley, H., Banks, J., Marsham, J. H., McQuaid, J. B., Sodemann, H., and Washington, R.: Optical properties of Saharan dust aerosol and contribution from the coarse mode as measured during the Fennec 2011 aircraft campaign, Atmos. Chem. Phys., 13, 303–325, doi:10.5194/acp-13-303-2013, 2013.

Scott, N. A. and Chédin, A.: A fast line-by-line method for atmospheric absorption computations: the automatized atmospheric absorption atlas, J. Appl. Meteor., 20, 802–812, 1981.

Shao, Y., Wyrwoll, K., Chappell, A., Huang, J., Lin, Z., McTainsh, G. H., Mikami, M., Tanaka, T. Y., Wang, X., and Yoon, S.: Dust cycle: an emerging core theme in earth system science, Aeolian Res., 2, 181–204, doi:10.1016/j.aeolia.2011.02.001, 2011.

Singh, R. P., Dey, S., Tripathi, S. N., Tare, V., and Holben, B.: Variability of aerosol parameters over Kanpur, northern India, J. Geophys. Res., 109, D23206, doi:10.1029/2004JD004966, 2004.

Smirnov, A., Holben, B. N., Dubovik, O., O'Neill, N. T., Eck, T. F., Westphal, D. L., Goroch, A. K., Pietras, C., and Slutsker, I.: Atmospheric aerosol optical properties in the Persian Gulf, J. Atmos. Sci., 59, 620–634, 2002.

Sokolik, I. N. and Toon, O. B.: Incorporation of mineralogical composition into models of the radiative properties of mineral aerosol from UV to IR wavelengths. J. Geophys. Res., 104, 9423–9444, 1999.

Sokolik, I., Toon, O. B., and Bergstrom, R. W.: Modeling the radiative characteristics of airborne mineral aerosols at infrared wavelengths, J. Geoph. Res., 103, 8813–8826, 1998.

Stamnes, K., Tsay, S.-C., Wiscombe, W., and Jayaweera, K.: Numerically stable algorithm for discrete ordinate-method radiative transfer in multiple scattering and emitting layered media, Appl. Optics, 27, 2502–2509, 1988.

Tanré, D., Haywood, J., Pelon, J., Léon, J.-F., Chatenet, B., Formenti, P., Francis, P., Goloub, P., Highwood, E., and Myhre, G.: Measurement and modeling of the Saharan dust radiative impact: overview of the Saharan Dust Experiment (SHADE), J. Geophys. Res., 108, 8574, doi:10.1029/2002JD003273, 2003.

Taylor, K. E.: Summarizing multiple aspects of model performance in a single diagram, J. Geophys. Res., 106, 7183–7192, 2001.

Tsamalis, C., Chédin, A., Pelon, J., and Capelle, V.: The seasonal vertical distribution of the Saharan Air Layer and its modulation by the wind, Atmos. Chem. Phys. Discuss., 13, 4727–4784, doi:10.5194/acpd-13-4727-2013, 2013.

US Climate Change Science Program: Atmospheric aerosol properties and climate impacts, A report by the US Climate Change Science Program and the Subcommittee on Global Change Research, edited by: Chin, M., Kahn, R. A., and Schwartz, S. E., report, NASA, Washington DC, 128 pp., 2009.

Vogelmann, A. M., Flatau, P. J., Szczodrak, M., Markowicz, K. M., and Minnett, P. J.: Observations of large aerosol infrared forcing at the surface, Geophys. Res. Lett., 30, 1655, doi:10.1029/2002GL016829, 2003.

ACPD
13, 30143–30186, 2013

Volz, F. E.: Infrared refractive index of atmospheric aerosol substances, Appl. Optics, 11, 755–759, 1972.
Volz, F. E.: Infrared optical constants ammonium sulfate, Sahara dust, volcanic pumace and flyash, Appl. Optics, 12, 564–568, 1973.
Walters Sr., K. R., Sjoberg, W. F.: The Persian Gulf Region, A Climatological Study, US Marine Corps, 62 pp., available at: http://www.marines.mil/News/Publications/ELECTRONICLIBRARY/ElectronicLibraryDisplay/tabid/13082/Article/127213/fmfrp-0-54.aspx (last access: November 2013), 1990.
Wang, S. H., Lin, N. H., Chou, M. D., Tsay, S. C., Welton, E. J., Hsu, N. C., Giles, D. M., Liu, G. R., and Holben, B. N.: Profiling transboundary aerosols over Taiwan and assessing their radiative effects, J. Geophys. Res., 115, D00K31, doi:10.1029/2009JD013798, 2010.
Winker, D., Hunt, W., and McGill, M.: Initial performance assessment of CALIOP, Geophys. Res. Lett., 34, L19803, doi:10.1029/2007GL030135, 2007.
Winker, D. M., Vaughan, M. A., Omar, A. H., Hu, Y., Powell, K. A., Liu, Z., Hunt, W. H., and Young, S. A.: Overview of the CALIPSO mission and CALIOP data processing algorithms, J. Atmos. Ocean. Technol., 26, 2310–2323, doi:10.1175/2009JTECHA1281.1, 2009.
Winker, D. M., Pelon, J., Coakley Jr., J. A., Ackerman, S. A., Charlson, R. J., Colarco, P. R., Flamant, P., Fu, Q., Hoff, R., Kittaka, C., Kubar, T. L., LeTreut, H., McCormick, M. P., Megie, G., Poole, L., Powell, K., Trepte, C., Vaughan, M. A., and Wielicki, B. A.: The CALIPSO mission: a global 3-D view of aerosols and clouds, B. Am. Meteorol. Soc., 91, 1211–1229, doi:10.1175/2010BAMS3009.1, 2010.
Yu, H., Kaufman, Y. J., Chin, M., Feingold, G., Remer, L. A., Anderson, T. L., Balkanski, Y., Bellouin, N., Boucher, O., Christopher, S., DeCola, P., Kahn, R., Koch, D., Loeb, N., Reddy, M. S., Schulz, M., Takemura, T., and Zhou, M.: A review of measurement-based assessments of the aerosol direct radiative effect and forcing, Atmos. Chem. Phys., 6, 613–666, doi:10.5194/acp-6-613-2006, 2006.

Table 1. List of the 38 AERONET sites selected for this study: name, longitude (degree), latitude (degree), 3-letter code, elevation (in m), 500 nm coarse mode AOD data quality level.

Site	Long	Lat	Code	Z (m)	Lev
Abu_Al_Bukhoosh	53.146	25.495	AAB	24	1.5
Dhabi	54.383	24.481	DHB	15	2.0
Dhadnah	56.325	25.513	DHA	81	2.0
Kuwait_University	47.971	29.325	KuU	42	2.0
Mezaira	53.779	23.145	MEZ	204	2.0
Mussafa	54.467	24.372	MUS	10	2.0
Solar_Village	46.397	24.700	SVA	764	2.0
Hada_el-Sham	39.729	21.802	HAD	254	1.5
KAUST_Campus	39.102	22.304	KAU	11	2.0
Agoufou	−1.479	15.345	AGO	305	1.5
Banizoumbou	2.665	13.541	BAN	250	1.5
Dakar	−16.959	14.394	DAK	0	2.0
DMN_Maine_Soroa	12.023	13.217	MaS	350	1.5
Tamanrasset_INM	5.530	22.790	TAM	1377	2.0
Zinder_Airport	8.990	13.777	ZiA	456	1.5
Zouerate-Fennec	−12.483	22.750	ZoF	343	1.5
Ilorin	4.340	8.320	ILO	350	2.0
CRPSM_Malindi	40.194	−2.996	MAL	12	1.5
Calhau	−24.867	16.864	CAL	40	1.5
Camaguey	−77.850	21.422	CAM	122	2.0
Capo_Verde	−22.935	16.733	CVE	60	2.0
Santa_Cruz_Tenerife	−16.247	28.473	TES	52	2.0
Izana	−16.499	28.309	TEI	2391	2.0
La_Laguna	−16.321	28.482	TEL	568	2.0
La_Parguera	−67.045	17.970	LPA	12	2.0
Ragged_Point	−59.432	13.165	BAR	40	2.0
Karachi	67.030	24.870	KAR	49	2.0
MCO-Hanimaadhoo	73.183	6.776	MCO	0	2.0
Pune	73.805	18.537	PUN	559	1.5
Jaipur	75.806	26.906	JAI	450	2.0
Gual_Pahari	77.150	28.426	GUA	384	2.0
Kanpur	80.232	26.513	KAN	123	2.0
Dhaka_University	90.398	23.728	DHU	34	1.5
GOT_Seaprism	101.412	9.286	GOT	10	1.5
Qiandaohu	119.053	29.556	QIA	133	1.5
EPA-NCU	121.185	24.968	NCU	144	2.0
Ningbo	121.547	29.860	NIN	121	1.5
Lucinda	146.386	−18.520	LUC	8	1.5

Discussion Paper | Discussion Paper | Discussion Paper | Discussion Paper |

ACPD
13, 30143–30186, 2013

Evaluation of IASI derived dust aerosols characteristics

V. Capelle et al.

Table 2. Correlation (last column) between IASI AOD and 500 nm coarse mode AERONET AOD over sea. Each site is identified by its name (1st column), its 3-digit code (2nd column), and identification number (3rd column). The 4th column gives the number of items in the statistics. The last line gives the overall statistics (all sites merged). An asterisk in the first column indicates that the AERONET coarse mode AOD data at this site are "Level 1.5" instead of "Level 2.0" (see text). Bold names correspond to stations with weak mean IASI AOD (all period average less than 0.08).

site	code	no	nb it	correl
Abu_Al_Bukhoosh*	AAB	1	12	0.67
Dhabi	DHB	2	7	0.87
Dhadnah	DHA	3	23	0.70
Kuwait_University	KuU	4	22	0.77
Mussafa	MUS	5	15	0.62
Solar_Village	SVA	6	48	0.83
KAUST_Campus	KAU	7	5	0.96
CRPSM_Malindi*	MAL	8	40	0.49
Calhau*	CAL	9	12	0.83
Camaguey	CAM	10	30	0.91
Capo_Verde	CVE	11	62	0.85
Dakar	DAK	12	25	0.74
Santa_Cruz_Tenerif	TES	13	44	0.80
Izana	TEI	14	49	0.86
La_Laguna	TEL	15	40	0.88
La_Parguera	LPA	16	43	0.86
Ragged_Point	BAR	17	49	0.77
Karachi	KAR	18	54	0.92
MCO-Hanimaadhoo	MCO	19	33	0.60
Pune*	PUN	20	47	0.81
Dhaka_University*	DHU	21	7	0.86
GOT_Seaprism*	GOT	22	6	0.72
EPA-NCU	NCU	23	26	0.65
Ningbo*	NIN	24	5	0.85
Lucinda*	LUC	25	8	0.67
All sites merged	av		713	0.88

ACPD
13, 30143–30186, 2013

ACPD
13, 30143–30186, 2013

Evaluation of IASI derived dust aerosols characteristics

V. Capelle et al.

Table 3. Same as for Table 2 except over land.

site	code	no	nb it	correl
Mezaira	MEZ	1	39	0.55
Solar_Village	SVA	2	51	0.48
Hada_el-Sham*	HAD	3	5	0.45
Agoufou*	AGO	4	39	0.64
Banizoumbou*	BAN	5	61	0.61
Dakar	DAK	6	25	0.73
DMN_Maine_Soroa*	MaS	7	28	0.55
Tamanrasset_INM	TAM	8	14	0.87
Zinder_Airport*	ZIN	9	43	0.55
Zouerate-Fennec*	ZoF	10	15	0.76
Ilorin	ILO	11	47	0.56
Karachi	KAR	12	57	0.81
Pune*	PUN	13	45	0.81
Jaipur	JAI	14	35	0.84
Gual_Pahari	GUA	15	12	0.82
Kanpur	KAN	16	55	0.61
Qiandaohu*	QIA	17	12	0.51
All sites merged	av		582	0.74

Table 4. Correlation (last column) between IASI and CALIOP altitude over sea. Each site is identified by its name (1st column), its 3-digit code (2nd column), and identification number (3rd column). The 4th column gives the number of items in the statistics. The last line gives the overall statistics (all sites merged).

site	code	no	nb it	correl
Abu_Al_Bukhoosh	AAB	1	40	0.62
Dhabi	DHB	2	40	0.62
Dhadnah	DHA	3	46	0.73
Kuwait_University	KuU	4	43	0.68
Mussafa	MUS	5	42	0.76
Solar_Village	SVA	6	44	0.76
KAUST_Campus	KAU	7	43	0.84
CRPSM_Malindi	MAL	8	40	0.35
Calhau	CAL	9	47	0.78
Camaguey	CAM	10	21	−0.05
Capo_Verde	CVE	11	47	0.78
Dakar	DAK	12	47	0.83
Santa_Cruz_Tenerif	TES	13	41	0.67
Izana	TEI	14	41	0.67
La_Laguna	TEL	15	41	0.67
La_Parguera	LPA	16	24	0.61
Ragged_Point	BAR	17	26	0.60
Karachi	KAR	18	45	0.76
MCO-Hanimaadhoo	MCO	19	44	0.80
Pune	PUN	20	44	0.79
Dhaka_University	DHU	21	39	0.51
GOT_Seaprism	GOT	22	28	0.17
EPA-NCU	NCU	23	30	0.52
Ningbo	NIN	24	12	0.33
Lucinda	LUC	25	15	−0.63
All sites merged	av		925	0.78

ACPD
13, 30143–30186, 2013

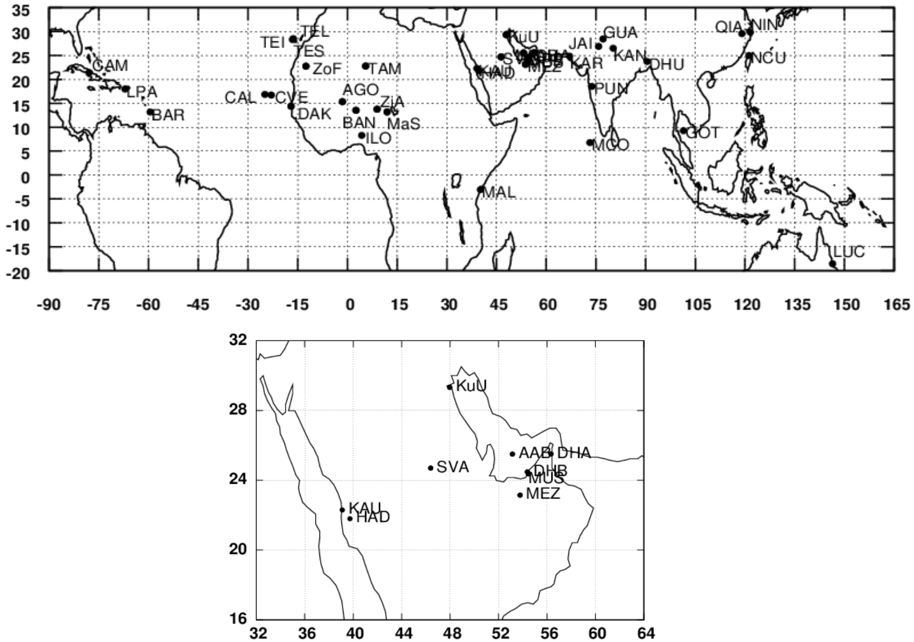

Fig. 1. Location of the 38 AERONET sites selected for this study. Top: whole tropical belt; bottom: zoom on the Arabian Peninsula. See Table 1 for the meaning of the 3-letter codes.

ACPD
13, 30143–30186, 2013

Evaluation of IASI derived dust aerosols characteristics

V. Capelle et al.

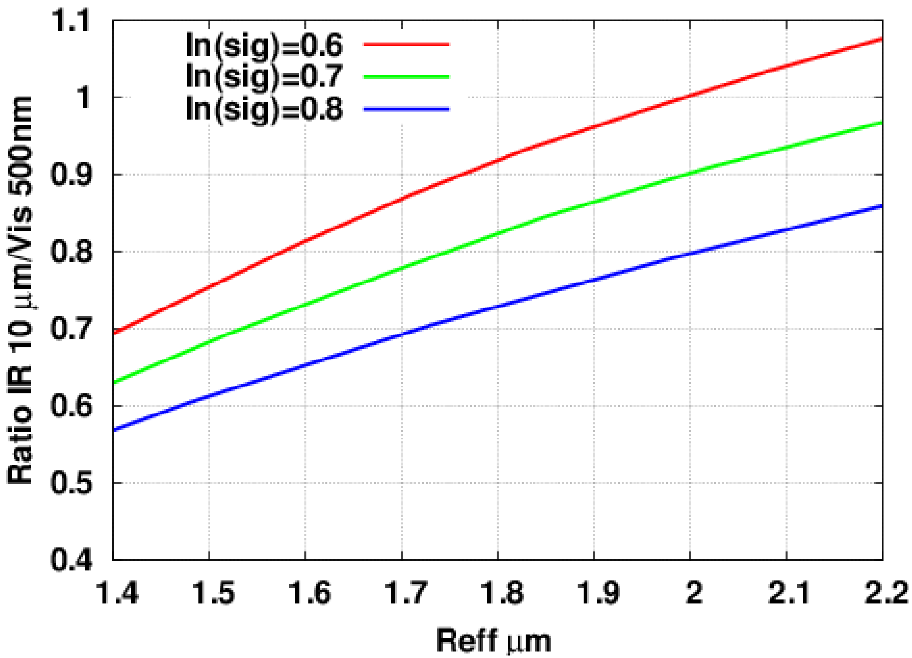

Fig. 2. Theoretical ratio IR 10 µm AOD/Visible coarse mode 500 nm AOD in function of the standard deviation of the width of the size distribution (ln(sig)) and of the effective radius (Reff).

ACPD
13, 30143–30186, 2013

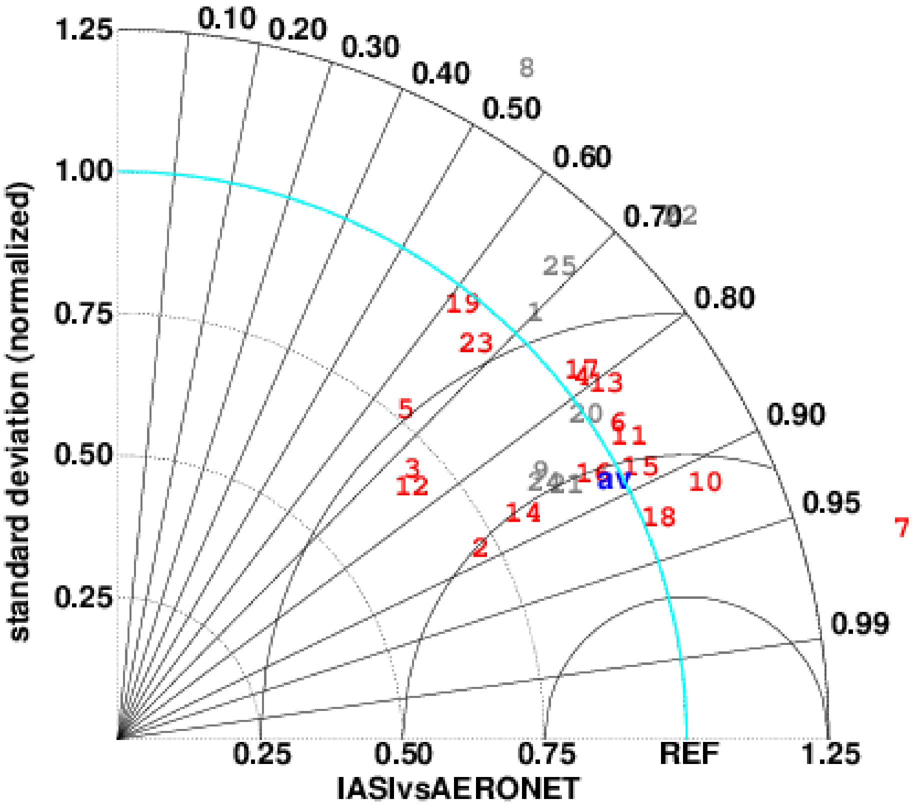

Fig. 3. Taylor diagram (normalized) for IASI and AERONET 500 nm coarse mode AOD over sea. Sites are identified by their number in Table 2. Grey numbers are for "Level 1.5" sites. The overall statistics appear in blue ("av" for average).

ACPD
13, 30143–30186, 2013

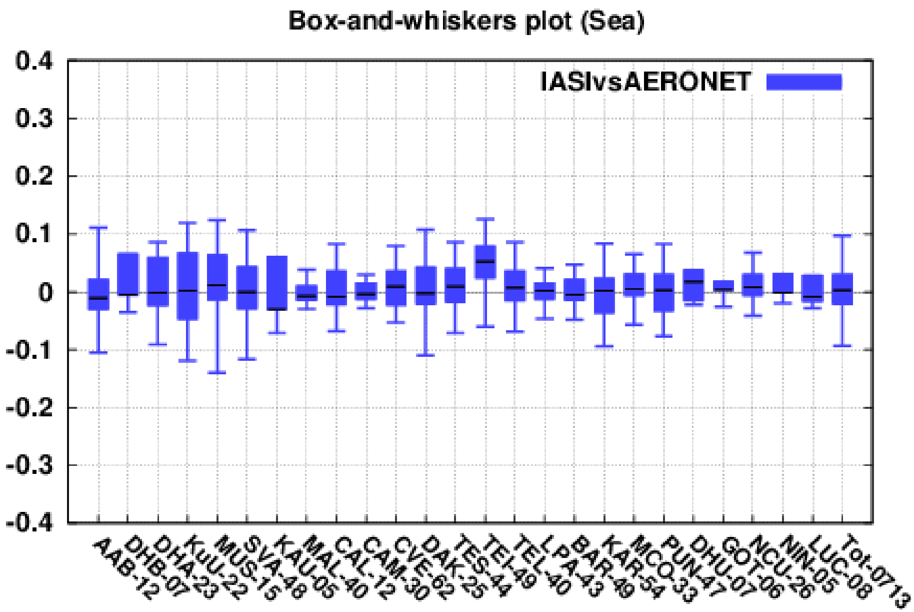

Fig. 4. Box-and-Whiskers plot (ends of the whiskers exclude the outliers) for the IASI and AERONET 500 nm coarse mode AOD over sea. Sites are identified by their code in Table 1, followed by the number of items. Last box marked "Tot": overall result.

ACPD
13, 30143–30186, 2013

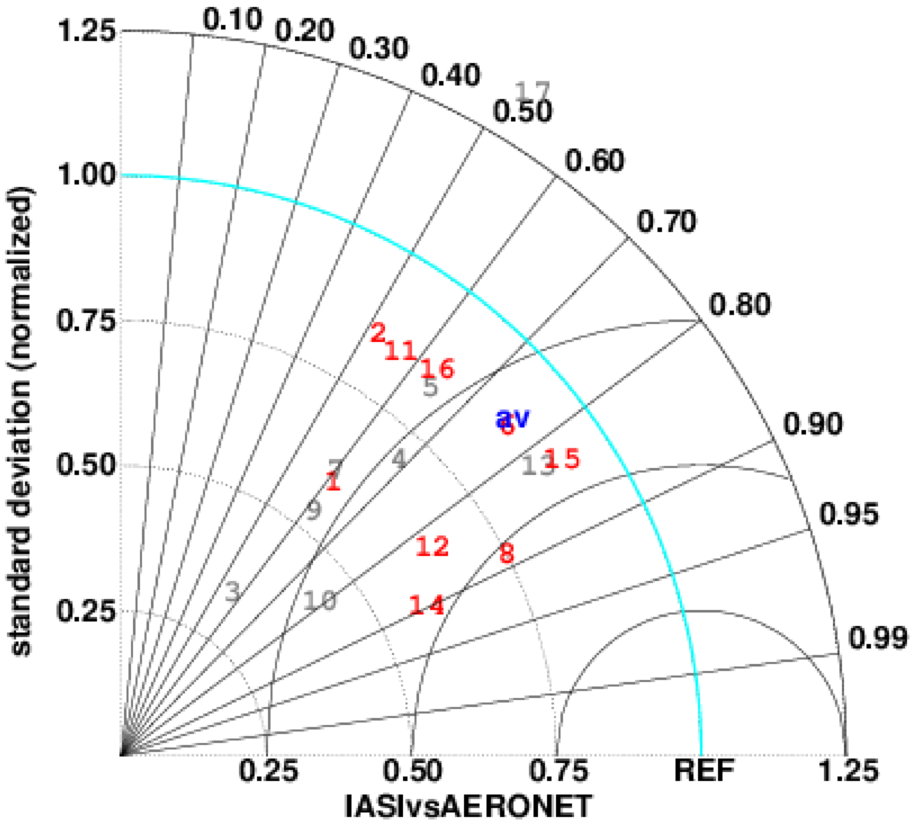

Fig. 5. Same as for Fig. 3 except over land.

ACPD
13, 30143–30186, 2013

Evaluation of IASI derived dust aerosols characteristics

V. Capelle et al.

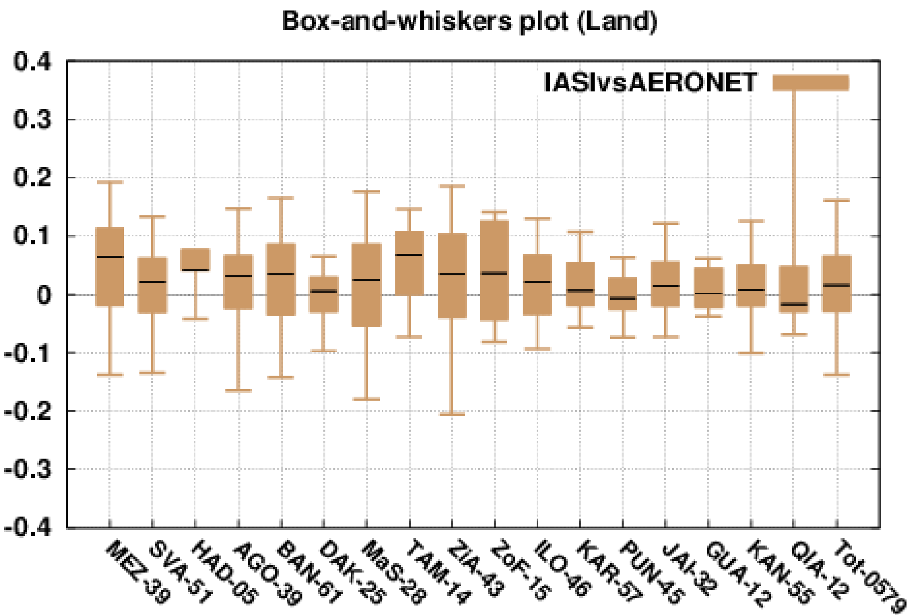

Fig. 6. Same as for Fig. 4 except over land.

ACPD
13, 30143–30186, 2013

Evaluation of IASI derived dust aerosols characteristics

V. Capelle et al.

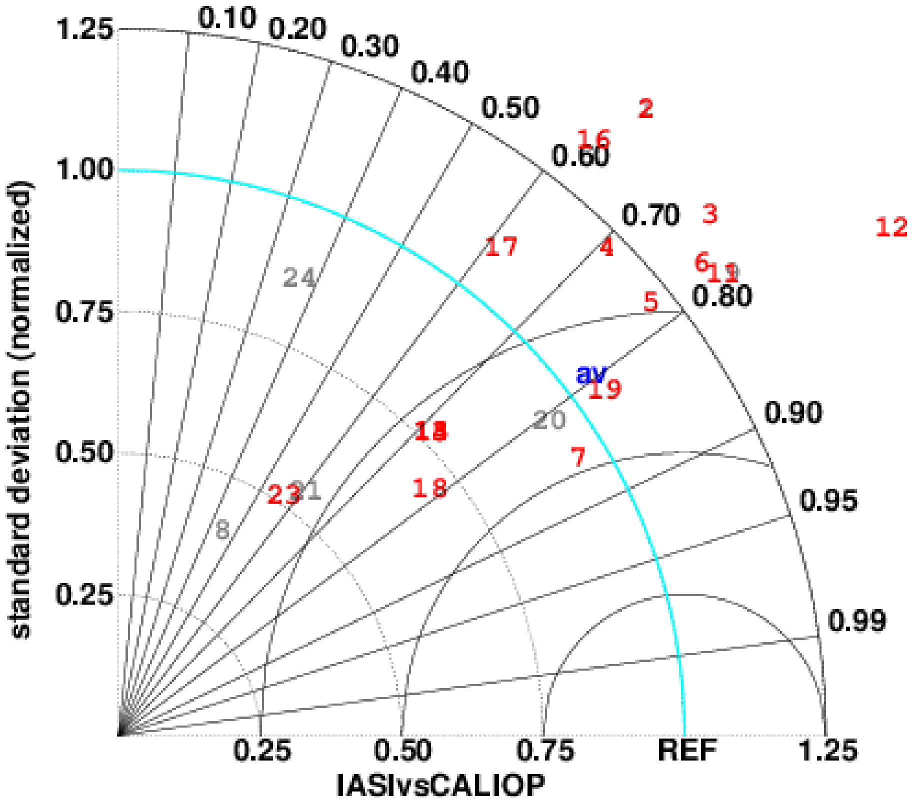

Fig. 7. Taylor diagram (normalized) for IASI and CALIOP altitude over sea. Sites are identified by their number in Table 2. The overall statistics appear in blue ("av" for average).

ACPD
13, 30143–30186, 2013

Evaluation of IASI derived dust aerosols characteristics

V. Capelle et al.

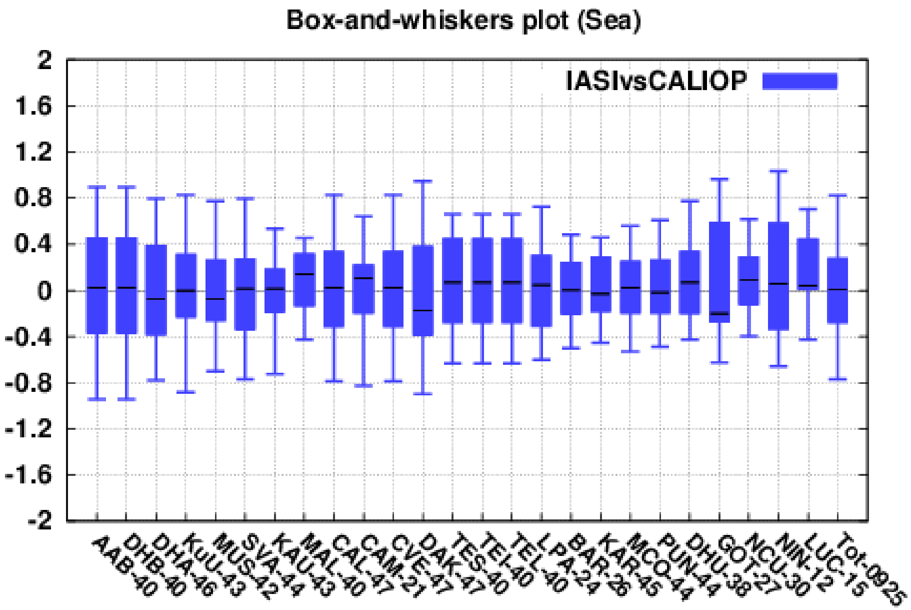

Fig. 8. Box-and-Whiskers plot (ends of the whiskers exclude the outliers) for the IASI and CALIOP altitude over sea. Y-axis in km. Sites are identified by their code in Table 1, followed by the number of items. Last box: overall result.

ACPD
13, 30143–30186, 2013

Evaluation of IASI derived dust aerosols characteristics

V. Capelle et al.

ACPD
13, 30143–30186, 2013

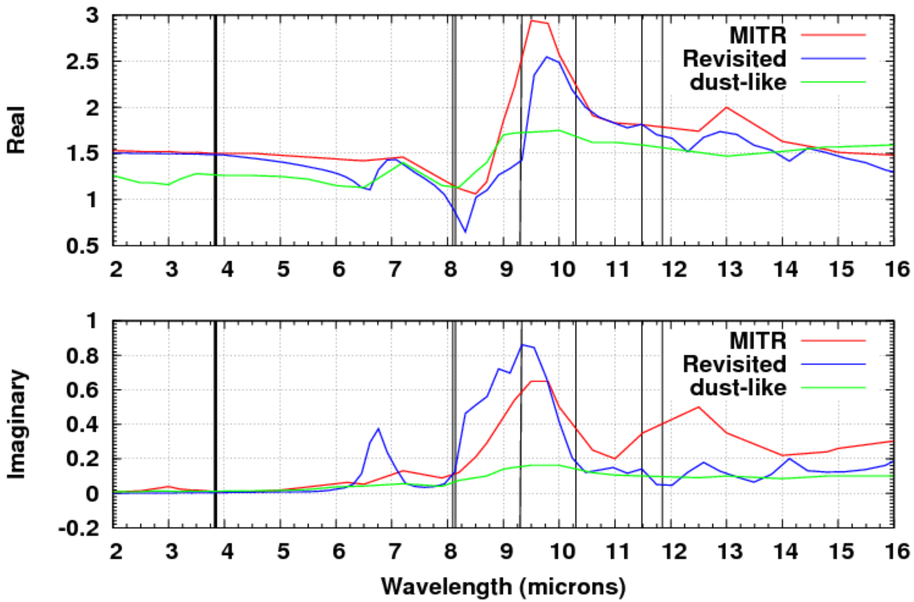

Fig. 9. Infrared real (top) and imaginary (bottom) refractive indices for "MITR" (Hess et al., 1998; Volz, 1973) in red, the "Revisited" IR from Balkanski et al. (2007) (0.9 % hematite) in blue, and "dust-like" from the measurements of Volz (1972, 1973) in green. Black vertical bars indicate the location of the IASI channels used to derive dust aerosol characteristics.

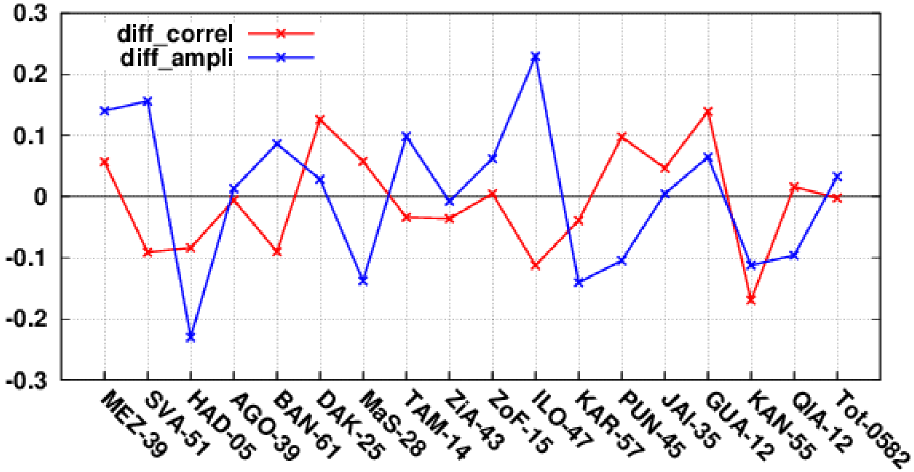

Fig. 10. Difference, site by site and total, between "MITR" and "Revisited" for the correlation (red) and the amplitude (normalized standard deviation; blue) for the AOD (IASI vs. AERONET). Positive (resp. negative) values mean larger correlation and amplitude closer to 1 (amplitude of the AERONET reference) for "MITR" (resp. "Revisited").

Discussion Paper | Discussion Paper | Discussion Paper | Discussion Paper |

ACPD

13, 30143–30186, 2013

Evaluation of IASI derived dust aerosols characteristics

V. Capelle et al.

Title Page
Abstract Introduction
Conclusions References
Tables Figures
◀I ▶I
◀ ▶
Back Close
Full Screen / Esc
Printer-friendly Version
Interactive Discussion